5-1-2011

Biokinetic Mechanisms Linked With Musculoskeletal Health Disparities: Stochastic Models Applying Tikhonov's Theorem to Biomolecule Homeostasis.

Asit K. Saha

Yu Liang

Sean S. Kohles
Portland State University

Biokinetic Mechanisms Linked With Musculoskeletal Health Disparities: Stochastic Models Applying Tikhonov's Theorem to Biomolecule Homeostasis

Asit K. Saha,
Center for Allaying Health Disparities through Research and Education (CADRE), Department of Mathematics & Computer Science, Central State University, Wilberforce, OH 45384

Yu Liang, and
Center for Allaying Health Disparities through Research and Education (CADRE), Department of Mathematics & Computer Science, Central State University, Wilberforce, OH 45384

Sean S. Kohles
Regenerative Bioengineering Laboratory, Department of Mechanical & Materials Engineering, Portland State University, Portland, OR 97207; Department of Surgery, Oregon Health & Science University, Portland, OR 97239

Asit K. Saha: asaha@centralstate.edu; Yu Liang: yliang@centralstate.edu; Sean S. Kohles: kohles@cecs.pdx.edu

Abstract

Multiscale technology and advanced mathematical models have been developed to control and characterize physicochemical interactions, respectively, enhancing cellular and molecular engineering progress. Ongoing tissue engineering development studies have provided experimental input for biokinetic models examining the influence of static or dynamic mechanical stimuli (Saha, A. K., and Kohles, S. S., 2010, "A Distinct Catabolic to Anabolic Threshold Due to Single-Cell Nanomechanical Stimulation in a Cartilage Biokinetics Model," J. Nanotechnol. Eng. Med., **1**(3) p. 031005; 2010, "Periodic Nanomechanical Stimulation in a Biokinetics Model Identifying Anabolic and Catabolic Pathways Associated With Cartilage Matrix Homeostasis," J. Nanotechnol. Eng. Med., **1**(4), p. 041001). In the current study, molecular regulatory thresholds associated with specific disease disparities are further examined through applications of stochastic mechanical stimuli. The results indicate that chondrocyte bioregulation initiates the catabolic pathway as a secondary response to control anabolic processes. In addition, high magnitude loading produced as a result of stochastic input creates a destabilized balance in homeostasis. This latter modeled result may be reflective of an injurious state or disease progression. These mathematical constructs provide a framework for single-cell mechanotransduction and may characterize transitions between healthy and disease states.

1 Introduction

Many musculoskeletal diseases, involving joints, muscles, bones, and connective tissues, are chronic and may cause life-long pain, disability, deformity, or even be fatal. These diseases afflict millions of Americans and cause tremendous suffering. Many of these diseases affect women and minorities disproportionately—both in increased numbers and increased severity. A mission of the National Institute of Arthritis and Musculoskeletal and Skin

Diseases (NIAMS) within the National Institutes of Health (NIH) is to support research into the causes, treatment, and prevention of arthritis and musculoskeletal diseases in order to reduce health disparities among racial and ethnic minorities.[2]

Diseases such as systemic lupus erythematosus, scleroderma, osteoarthritis, and keloids are included in the operational goals of NIAMS as those in which a health disparity has been clearly identified. These conditions have one thing in common in that the end-result involves dysfunction and destruction of the connective tissue, with eventual loss of the affected tissues as a therapeutic approach. As a component of addressing disparity and prevention, it will be important to identify biomarkers associated with these diseases. As valid indicators of disease, biomarkers may serve as candidate surrogate end points in clinical trials addressing therapeutic interventions.

To get an accurate identification of appropriate biomarkers, understanding the physiologic, anatomic, and biochemical parameters at each sequential event that leads to various disease stages will be important. As such, the research problem related to these connective tissue diseases is highly multidisciplinary and resolved at multiple scales. International collaborations have taken a wide variety of approaches to solve these complex problems, each with varied success.

The approach described herein takes the top to bottom approach in order to understand the complex biodynamics by starting at the tissue level. The goals of this effort are to advance the fundamental understanding of biological and chemical systems, to broaden the basic knowledge of the biomolecular interactions, and to translate this information into innovative designs supporting the engineering of novel biomaterials, devices, and processes. This effort will also help to clarify healthy physiologic dynamics and the biochemical parameters influencing native and engineered tissues with the primary purpose of minimizing the health disparity among certain communities and ethnic groups, mainly that of African Americans.

For the modeled musculoskeletal system here, the focus is on articular cartilage, a remarkably complex biocomposite material that exhibits outstanding compressive stiffness, toughness, and strength, resiliency, and shock absorption. The extracellular matrix (ECM) of mature articular cartilage contains approximately 60% collagen, 25% proteoglycans (PG), and 15% of a wide range of matrix proteins. The architectural collagen network provides a mechanical framework and is considered a structural molecule. PG is a central protein core to which sulfated glycosaminoglycans (GAG) composed of chondroitin sulfate, dermatan sulfate and keratan sulfate, are covalently attached, in a hydrophilic network. The single chondrocyte phenotype is distributed sparsely within the ECM. The third type of biomolecule in ECM includes a wide range of proteins such as different types of growth factors, fibronectin, laminin, and cytokines [1].

The physiologic regulation and the biologic integrity of cartilage tissue biomolecules are maintained by the chondrocytes, even though low in number and sparsely distributed [2,1,3]. Due to its location at the joint surfaces, articular cartilage experiences a wide range of forces that include shear, compression, and tension. These mechanical loads are distributed throughout the cartilage matrix and absorbed by the cartilage biomolecules. At the nanoscale, the mechanical stimulations are then dissipated and transmitted to chondrocytes. Understanding the structure, function, and regulation of the chondrocytes in real time at the nanoscale is a challenging task.

In normal and pathological conditions, articular cartilage matrix homeostasis is dependent on autocrine and paracrine regulatory mechanisms. These mechanisms are governed by anabolic and catabolic pathways, as controlled by the chondrocytes [4,5]. Chondrocytes produce the articular cartilage structural macromolecules, such as collagen and proteoglycans, which helps tissue formation and remodeling. Concomitantly, the cells produce a variety of metalloproteinases, such as collagenase, gelatinase, stromelysin, and aggrecanase, which are responsible for tissue turnover [6–8]. During healthy balanced regulation, growth factors such as transforming growth factor -β (TGF-β), insulinlike growth factor-1 (IGF-1), and osteogenic protein-1 (OP-1) stimulate the chondrocytes to synthesis the structural macromolecules (anabolic pathways), while cytokines interleukin-1 (IL-1), interleukin-6 (IL-6), and tumor necrosis factor-α (TNF-α), stimulate chondrocyte secretion of proteinases causing ECM degradation (catabolic pathways).

From a system science point of view, it is now clear that growth, maintenance, and degradation of the cartilage matrix are dependent on a balance between anabolic and catabolic activities. These relationships have been observed in controlled osteoarthritic culture models where experimental results show that the combination of anabolic growth factors and protective catabolic blockers may be a means for partial restoration of the cartilage matrix [9]. Reported results suggest that excessive release of basic fibroblast growth factors (bFGFs) from the cartilage matrix during injury, excessive loading, or osteoarthritis could contribute to increased proliferation and reduced anabolic activities in articular cartilage [10,11]. Previous predictions based on system dynamics modeling suggest that articular cartilage matrix synthesis clearly indicate that anabolic actions of different growth factors are essentially dose and time dependent [12,13]. In addition, applied mechanical stresses play an important role in healthy cartilage maintenance [6,7,14].

At the nanoscale, the dissipated mechanical stresses activate the cell to molecule interaction that enhances the controlled regulatory network of anabolic and catabolic pathways toward matrix homeostasis. Previously, a biokinetic model with static mechanical loading identified a transitional threshold load level from which the mechanical input caused a shift from a catabolic state to an anabolic state [6]. The modeled molecule homeostatic levels appeared to be dependent on the mechanical stimulus as seen experimentally within a controlled microenvironment [15,16]. Further model iterations identified a system dynamics mechanism balancing the harmony between catabolic and anabolic states [7]. Relative applied load limits were able to distinguish between "healthy" and "injurious" biomolecule accumulations within the modeled microenvironment.

In the present study, a system dynamics model further explores the multiscale cellular-biomolecular response within an unpredicted microenvironment through stochastic fluctuations in mechanical loading. The objective here is to characterize the biokinetic balance achieved through randomly imposed mechanical loading with respect to time as a further identification of the degenerative biomolecular interplay associated with musculoskeletal health disparities.

2 Materials and Methods

2.1 Mathematical Model Development

The foundation of the presented model involves anabolic/catabolic pathways that maintain ECM structural molecule depositions as previously summarized [6–8]. Briefly, many of the same mathematical functions are utilized with modifications incorporating the probabilistic nature of microbioenvironments. The schematic diagram of the system network adapted from our previous work indicates the feedback relationships adapted here for three time scales (Fig. 1).

A probabilistic or unpredictable component of the microenvironment can be coupled with the previous models by incorporating a Gaussian white noise function with small amplitudes. Theoretically, the random mechanical loading can influence all interactive dynamics and/or all of the biomolecules. For simplicity, the nanoscale aspect of the randomly generated mechanical loading is assumed to act only on the cytokine and growth factor dynamics.

The previous mathematical model described anabolic and catabolic regulation through growth factor (G) and cytokine (C) abundance along with collagen and GAG deposition as follows:

$$\frac{d[C]}{dt} = \eta_1[C]\{\Re_2 - [G]\} - \mu_1[C]$$
$$\frac{d[C]}{dt} = \eta_2[G]\{[C] - \Re_1\} - \mu_2[G]$$
$$\frac{d[\text{collagen}]}{dt} = \frac{v_2[G]}{K^{-1}+[C]} - \sigma_1[\text{collagen}]$$
$$\frac{d[\text{GAG}]}{dt} = \frac{v_2[G]}{K^{-1}+[C]} - \sigma_2[\text{GAG}]$$

(1)

where η_i = growth rates, μ_i = natural degradation rates, v_i = growth rates for ECM structural molecules production, σ_i = natural degradation rate of ECM structural molecules, K=saturation parameter, and $\Re_i$ = pivotal concentration, for (i=1,2), and 1=cytokines and 2=growth factors.

The challenges in quantitatively designing system dynamics processes mainly reside in the complex multiscale structures, which are extremely difficult to analyze by an averaging or classical approach. From reported experimental observations, one can see that the dynamics of cartilage biology operates at multiple time and geometric scales. In order to capture the dynamics of structure and function at the most natural levels, identification of those scales is key. The dynamic nature of biological structures at all scales makes it extremely complicated to accurately model systems without making a feasible connection between these scales. It is also important that dynamics at the nanoscale create evolving properties at the larger scales that are important for accurate simulations. Changes in the dynamics at one scale may change the fundamental parameters of a simulation at another scale. Failure to distinguish these parameters can limit the accuracy of the simulations [17]. From the reported data, it may be observed that the growth kinetics of cytokines and growth factors are very rapid compared with other biomolecules in the ECM. This relationship suggests that cartilage dynamics at the nano- or molecular level may have different time scales than that of higher order geometries. This phenomenon is indicated in the three-dimensional network schematic where each plane represents a different time scale (Fig. 1).

In order to incorporate the scale-phenomenon we rescaled the mathematics (Eq. (1)) into the canonical form:

$$\frac{1}{K}\frac{dC}{dT} = \alpha_1 C(\Omega_2 - G) - \beta_1 C$$
$$\frac{1}{K}\frac{dG}{dT} = \alpha_2 G(C - \Omega_1) - \beta_2 G$$

(2)

$$\frac{d}{dT}(\text{GAG}) = \frac{\lambda_1 G}{1+C} - \delta_1(\text{GAG})$$
$$\frac{d}{dT}(\text{collagen}) = \frac{\lambda_2 G}{1+C} - \delta_2(\text{collagen})$$

(3)

The scaling factors for the mathematical systems (2) and (3) are then

$$C=K[C], \quad G=K[G], \quad E=K^{-1}[E], \quad T=K^{-3}[t]$$
$$\alpha_1=K\eta_1, \quad \alpha_2=K\eta_2, \quad \beta_1=K^2\mu_1, \quad \beta_2=K^2\mu_2,$$
$$\Omega_1=K\mathfrak{R}_1, \quad \Omega_2=K\mathfrak{R}_2$$

for 1=cytokines and 2=growth factors, as noted previously, and

$$\lambda_{i,j}=K^2\upsilon_{i,j}, \quad \delta_{i,j}=K^3\sigma_{i,j} \tag{4}$$

for i, j =1,2, where 1=GAG and 2=collagen (see Table 1). The entire system can now be viewed as two subsystems:

$$\varepsilon\frac{d}{dT}\left(\begin{array}{c} C \\ G \end{array}\right)=\left(\begin{array}{c} f_1(C,G,\alpha_1,\beta_1,\Omega_2) \\ f_2(C,G,\alpha_2,\beta_2,\Omega_1) \end{array}\right) \tag{5}$$

$$\frac{d}{dT}\left(\begin{array}{c} \text{GAG} \\ \text{collagen} \end{array}\right)=\left(\begin{array}{c} \frac{\lambda_1 G}{1+C} - \delta_1(\text{GAG}) \\ \frac{\lambda_2 G}{1+C} - \delta_2(\text{collagen}) \end{array}\right) \tag{6}$$

where

$$\varepsilon=\frac{1}{K}$$
$$f_1(C,G,\alpha_1,\beta_1,\Omega_2)=\alpha_1 C(\Omega_2 - G) - \beta_1 C$$
$$f_2(C,G,\alpha_2,\beta_2,\Omega_1)=\alpha_2 G(C - \Omega_1) - \beta_2 G \tag{7}$$

In order to solve these interlinked differential equations over multiple scales and parameters, a specialized analytical technique may be applied that of Tikhonov's theorem [18].

2.2 Application of Tikhonov's Theorem

Consider the system

$$\frac{dx}{dt}=f(x, y)$$
$$\zeta\frac{dy}{dt}=g(x, y) \tag{8}$$

where $x \in R^n$, $y \in R^m$, and $\zeta>0$ is a small parameter. Assume that there exists a solution $y = \psi(x)$ of the system, when $g(x,y) =0$, with the stipulations: (1) if the solution is isolated and positively stable in a closed bounded domain $D \subset R^n$, (2) if the initial point $(x(0), y(0))$ belongs to the domain of influence within this solution, and (3) if the solution of the degenerated system, $dx/dt = f(x, \psi(x))$, belongs to D for $0 \le t \le T$, then (4) the solution $(x(t, \zeta), y(t, \zeta))$ of the actual system (8) tends toward the solution $(\bar{x}(t), \bar{y}(t))$ of the degenerated system $dx/dt = f(x, \psi(x))$, as $\zeta \to 0$.

Applying this theorem to our system (5) and (6), it was observed that when $\varepsilon \to 0$ as $K \to + \infty$, the positively stable and isolated solution becomes

$$\begin{pmatrix} \overline{C} \\ \overline{G} \end{pmatrix} = \begin{pmatrix} \Omega_1 + \frac{\beta_2}{\alpha_2} \\ \Omega_2 - \frac{\beta_1}{\alpha_1} \end{pmatrix}$$

(9)

for the system

$$\begin{pmatrix} f_1(C, G, \alpha_1, \beta_1, \Omega_2) \\ f_2(C, G, \alpha_2, \beta_2, \Omega_1) \end{pmatrix} = 0$$

(10)

As shown in the schematic diagram, the system experiences a mechanical stress as a biologically realistic phenomenon. Since cartilage is a low-friction, load-bearing surface, it experiences a range of static and dynamic loads that include shear, compression, and tension. These mechanical loadings are absorbed by the ECM and then are dispersed to the chondrocytes. The chondrocytes then convert these mechanical signals into biochemical signals, which then arbitrate both the anabolic and catabolic pathways. The developed solution will provide a mathematical means to translate mechanical signals to biochemical signals and trigger the two fundamental pathways for matrix homeostasis.

In this model, the unknown dynamics associated with mechanical loading is incorporated as random (stochastic) loading on the anabolic and catabolic pathways through a perturbation of the growth factors and cytokines. Hence, the mathematical model with random mechanical loading at the molecular level becomes

$$\frac{1}{K} d \begin{pmatrix} C \\ G \end{pmatrix} = \begin{bmatrix} \alpha_1 C (\Omega_2 - G) - \beta_1 C \\ \alpha_2 G (C - \Omega_1) - \beta_2 G \end{bmatrix} dt + \begin{pmatrix} \rho_{CC} & \rho_{CG} \\ \rho_{GC} & \rho_{GG} \end{pmatrix} \vartheta dW_t$$

(11)

where ϑdW_t is the Weiner process [19]. Here, ρ_{CC} is the scaling factor when randomly generated mechanical stress is directly acting on the catabolic pathways, ρ_{CG} is the cross-scaling factor when the randomly generated mechanical stress is directly acting on anabolic pathways that influence catabolic pathways, ρ_{GC} is the cross-scaling factor when randomly generated mechanical stress is directly acting on catabolic pathways that influence anabolic pathways, and ρ_{GG} is the scaling factor when randomly generated mechanical stress is directly acting on anabolic pathways. ϑ is the scaling factor that arises from the random number generation.

The second half of the system describes the synthesis of the main ECM molecules, GAG, and collagen, where growth factors enhance production and cytokines inhibit production through the negative feedback control mechanism:

$$\frac{d}{dt}(\text{GAG}) = \frac{\lambda_1 G}{1 + C} - \delta_1(\text{GAG})$$
$$\frac{d}{dt}(\text{collagen}) = \frac{\lambda_2 G}{1 + C} - \delta_2(\text{collagen})$$

(12)

The mathematical systems are now formulated for experimental boundary conditions representing engineered tissue development.

2.3 Bioregulatory Simulation

Normalized parameter estimations associated with anabolic and catabolic pathways within an engineered cartilage tissue environment are limited in availability. Therefore, a mathematical association between growth factor and cytokine abundance was drawn from data characterizing the development of sweat glands in human fetal skin [20]. This tissue source facilitated an initial parametric relationship [8]. Although physiologically unrelated to cartilage, the data represent the synergistic effects of cytokines and growth factors over a time-frame typical for recent engineered cartilage culture scenarios [14]. The assumed intrinsic GAG and collagen kinetic rates associated with both growth factor and cytokine influence were defined in previous mechanistic [21], deterministic, and stochastic [12,13] models (Table 1).

As mentioned for the deterministic system (5) and (6), when $1/K \to 0$ as $K \to +\infty$, the positively stable and isolated solution exists, $y = \psi(x)$. Tikhonov's theorem as developed for the stochastic differential equation system described in Eqs. (12) can be applied here. As the system (12) is random in nature, the isolated and positively stable solution

$$\begin{pmatrix} \overline{C} \\ \overline{G} \end{pmatrix} = \begin{pmatrix} \Omega_1 + \frac{\beta_2}{\alpha_2} \\ \Omega_2 - \frac{\beta_1}{\alpha_1} \end{pmatrix} \tag{13}$$

can be replaced by

$$\begin{pmatrix} \overline{C} \\ \overline{G} \end{pmatrix} = \begin{pmatrix} \text{mean value of cytokines} \\ \text{mean value of growth} - \text{factor} \end{pmatrix} \tag{14}$$

The two pivotal threshold parameters Ω_1 and Ω_2 provide an interplay and boundary as a vital role in the growth kinetics of catabolic and anabolic pathways. Chondrocyte control over the matrix homeostasis partly depends on these two parametric values via the intensity of the fundamental kinetics (Fig. 2). Applying linear programming methodology, the relationships

$$2.6720 \leq \Omega_2 - \Omega_1 \leq 4.6720 \tag{15}$$

were defined as boundary conditions for typical engineered tissue methodologies.

2.4 Discretizing the Stochastic Differential Equation

The dynamic system as described in Eq. (11) is a stochastic differential equation (SDE). It is extremely difficult to get an explicit solution of a multidimensional SDE. A discretization scheme may the appropriate choice for finding the solution trajectories of a SDE. As the diffusion coefficient is deterministic, we adapt an Euler type discretization scheme for our system here [22]:

$$\boldsymbol{X}_{s+\Delta s}(w) = \boldsymbol{X}_s(w) + \boldsymbol{F}(\boldsymbol{X}_s(w))\Delta s + \boldsymbol{\Psi}(\boldsymbol{X}_s(w))(W_{s+\Delta s}(w) - W_s(w)) \tag{16}$$

with a deterministic initial condition $\boldsymbol{X}_0(w) = \boldsymbol{x}_0$, where

$$X_t(w) = \begin{pmatrix} C_t(w) \\ G_t(w) \end{pmatrix}$$

(17)

and

$$F(X_t(w)) = \begin{pmatrix} \alpha_1 C_t(w)(\Omega_2 - G_t(w)) - \beta_1 C_t(w) \\ \alpha_2 G_1(w)(C_t(w) - \Omega_1) - \beta_2 G_t(w) \end{pmatrix}$$

(18)

and

$$\Psi(X_s(w)) = \begin{pmatrix} \rho_{CC} & \rho_{CG} \\ \rho_{GC} & \rho_{GG} \end{pmatrix} = \text{const}$$

(19)

The stochastic term, $(W_{s+\Delta s}(w) - W_s(w))$, is approximated by the random number generated by the pseudorandom values drawn from the standard uniform distribution on the open interval (0, 1). The initial condition was assumed to be

$$X_0(w) = \begin{pmatrix} 0.618 \\ 0.4 \end{pmatrix}$$

(20)

as input for simulation of the system (11) using the above scheme (14).

In a modification of Tikhonov's theorem, the solution $(x(t, \zeta), y(t, \zeta))$ of the actual system (8) tends toward the solution $(\bar{x}(t), \bar{y}(t))$ of the degenerated system $dx/dt = f(x, \psi(x))$, as $\zeta \to 0$. Using this concept and the assumption given in Eq. (13), the following multiscale aspects of GAG and collagen accumulation are defined (due to multiscale cytokines and growth factors, $\bar{C}$ and $\bar{G}$, respectively):

$$\frac{d}{dt}(\text{GAG}) = \frac{\lambda_1 \bar{G}}{1+\bar{C}} - \delta_1(\text{GAG})$$
$$\frac{d}{dt}(\text{collagen}) = \frac{\lambda_2 \bar{G}}{1+\bar{C}} - \delta_2(\text{collagen})$$

(21)

Hence, the steady state accumulation is given by

$$\begin{pmatrix} \overline{\text{GAG}_{ss}} \\ \overline{\text{collagen}_{ss}} \end{pmatrix} = \begin{pmatrix} \frac{1}{\delta_1}\left(\frac{\lambda_1 \bar{G}}{1+\bar{C}}\right) \\ \frac{1}{\delta_2}\left(\frac{\lambda_2 \bar{G}}{1+\bar{C}}\right) \end{pmatrix}$$

(22)

With these mathematical frameworks, Monte Carlo simulations were performed for 50,000 sample points with commercial software (MATLAB, Mathworks, Inc., Natick, MA).

3 Results

From the previous results examining single time scales, it was shown that lower magnitude mechanical loads have minimal impact on the harmonic balance between anabolic and catabolic pathways. This was demonstrated in deterministic models of these interaction pathways due to static and periodic loads [6,7]. In the current work, phase-plane dynamics of cytokines and growth factors are demonstrated graphically with respect to highly random mechanical loading with concentrations shown in relative units. Upon stratifying the stochastic input, the lower to higher relative load values of 0.001, 0.01, and 0.1, respectively, are tending to push the clockwise oscillations between cytokines and growth factors toward a slight growth factor bias (Fig. 3).

A breakdown in the cyclic relationship between anabolic and catabolic pathways is observed when the random load value increases to ≥0.5 (Fig. 4). Hence, the observation is made that random loading at near 0.5 relative units is the starting point of homeostatic destabilization of the cyclical trajectory of the anabolic and catabolic pathways. In order to understand the physical relevance of this result, the resulting sample data are gathered from the Monte Carlo simulation. Here, a variance analysis describes the standard deviation at each load level for cytokine and growth factor concentrations, where a load level of ~0.5 represents an inflection point in concentration precision (Fig. 5). This result indicates an ordinal relationship in the biokinetics such that the catabolic pathway follows the anabolic pathway. In the current model structure, a reversal of the sequence could not be produced.

When exploring a possible third mechanism for controlling cellular catabolism, the application of a random load application much higher than ~0.5 and ($SD_{cytokines}-SD_{growth\_factor}$) <0 causes the phase-plane trajectory to show some chaotic behavior (Fig. 6). In this scenario, the anabolic pathway takes control over the catabolic pathway. As the random mechanical load continues to increase, a complicated chaotic trajectory of cytokines and growth factor in the phase-plane is evident (Fig. 6). The system fails to generate a feasible trajectory when random mechanical loading is over 65 (Fig. 7). Excessive tissue generation may be evident at high load levels, indicating an injurious or disease state.

Finally, the mean magnitudes of GAG and collagen molecule accumulation are shown at different random mechanical load levels (Fig. 8). As the system is now multiscaled, the cytokine and growth factor influence ($\bar{C}$ and $\bar{G}$ in Eq. (22)) is also multiscale.

4 Discussion

In this present paper, we considered the applied mechanical forces on cartilage tissue as being random in nature. A driving motivation is to assess the random nature of any mechanical stimulus actually transferring a mechanical signal to the tissue subsystems (cells, biomolecules, etc.). It remains unclear as to how exactly chondrocytes receive and adapt to these applied mechanical loadings. The presented approach provides a novel phenomenological model that may explain the effects of randomly generated mechanical loading within cartilage tissue. This phenomenological approach provides some explanation of the complex dynamics influencing cartilage mechanobiology. It is evident that a causal temporality is necessary in the feedback sequence, in that an anabolic pathway alone cannot influence the biologic system toward attaining matrix homeostasis. Based on our mathematical framework, the chondrocyte regulator initiates the catabolic pathway as a secondary response to control the anabolic pathway. This system dynamics approach has not yet been successful in proving the reverse order. Therefore, the simultaneous existence of both functions is absolutely necessary to maintain homeostasis, as we observed previously.

This research is framed with the purpose of elucidating biokinetic mechanisms linked with critical diseases inordinately affecting minority populations. Cartilage constituent abundance and organization (cells, GAG, collagen, etc.) can now be quantitatively explored as associated with these diseases. This may be evident in the chaotic nature of tissue synthesis/degradation when stochastic loading produces high magnitudes (Figs. 6 and 7). These diseases and their relevancy with the catabolic and anabolic processes include:

Lupus, a potentially fatal autoimmune disease, in which internal germ defensive systems attack its own tissues. This disease causes arthritis and damage to the kidney, heart, blood vessels, and the brain, affecting African American women at a threefold higher incidence and mortality rate than Caucasian women [23].

Scleroderma is classified as an autoimmune disease that occurs much more frequently in women than in men and is highly prevalent in certain Native Americans. Scleroderma is a chronic progressive disease in which occurs a thickening and scarring of the connective tissue due to excess deposits of collagen in the lungs, heart, kidneys, intestinal tract, joints, and muscles [24].

Osteoarthritis, a degenerative joint disease, noted to have a higher risk of both bilateral knee and hip osteoarthritis in African Americans than Caucasians. This disease is compounded by the additional risk factor of obesity [25].

Keloid scar is an abnormal exuberant form of wound healing in which excessive connective tissue is laid down at the wound site, and is not remodeled normally. This response can be distinguished from hypertrophic scars in which there is excess connective tissue initially, but remodeling takes place over time. Keloids are seen predominantly in African American individuals [26].

Researchers have suggested that mechanical forces do have some vital role in controlling and manipulating chondroctye behavior with respect to connective tissue remodelling and homeostasis, especially that possibly linked with the described diseases [27,28]. However, there is not much knowledge as to how these mechanical forces activate the chondrocytes when transitioning between healthy and disease states. Many types of mechanical forces are experienced during normal human activities. These can be static, dynamic (periodic), and random in nature. Whatever the pattern or mode of the applied mechanical force, a triggering influence on cartilage tissue health or disease is rectified at multiple scales.

Future modeling approaches will introduce the heterogenic nature of cartilage organization and the relationship with health maintenance or disease progression. It has been observed that physical movements and induced mechanical forces can maintain the health-state of a cartilage tissue as a contributing factor toward the heterogeneous structural organization of ECM [29,30]. A reduction in the geometric thickness of the cartilage tissue due to the absence of mechanical loading has also been observed [30]. With respect to cartilage organization, the concentration of lubricating molecules (such as lubricin) is highest at the articular surface, whereas higher concentrations of aggrecans are found in deeper zones [31,32]. During localized compression/tension, molecular deformation influences the flux of nutrients (imbibation and exudation) between the extracellular space and the synovial cavity [33–35]. This response can be considered as either a biphasic or triphasic composite mechanics phenomena with potential for enhancement as a systems biology perspective.

The results of the presented phenomenologic model describing a random loading environment support previous outcomes from deterministic models having static and dynamic loading conditions. The current SDE approach may explain why the complex kinetics of anabolic and catabolic pathways is not specifically sensitive to how the

mechanical loadings act, but rather that the amount of loading is within a small range. The chaotic nature of these pathways was observed when load ranges become moderately high. Overall these relationships shed additional light on mathematical constructs describing single-cell mechanotransduction.

Acknowledgments

References

1. Roughley PJ, Lee ER. Cartilage Proteoglycans: Structure and Potential Functions. Microsc Res Tech. 1994; 28:385–397. [PubMed: 7919526]

2. Caplan AI. Cartilage. Sci Am. 1984; 251(4):84–94. [PubMed: 6435245]

3. Buckwalter JA, Mankin HJ. Articular Cartilage, Tissue Design and Chondrocytes Matrix Interactions. Instructional Course Lectures. 1997; 47:477–486. [PubMed: 9571449]

4. Chambers MG, Bayliss MT, Mason RM. Chondrocyte Cytokine and growth factor expression in Murine Osteoarthritis. Osteoarthritis Cartilage. 1997; 5:301–308. [PubMed: 9497937]

5. Moos V, Fickert S, Muller B, Weber U, Sleper J. Immunohistological Analysis of Cytokine Expression in Human Osteoarthritic and Healthy Cartilage. J Rheumatol. 1999; 26:870–879. [PubMed: 10229409]

6. Saha AK, Kohles SS. A Distinct Catabolic to Anabolic Threshold Due to Single-Cell Static Nanomechanical Stimulation in a Cartilage Biokinetics Model. J Nanotechnol Eng Med. 2010; 1(3): 031005.

7. Saha AK, Kohles SS. Periodic Nanomechanical Stimulation in a Biokinetics Model Identifying Anabolic and Catabolic Pathways Associated With Cartilage Matrix Homeostasis. J Nanotechnol Eng Med. 2010; 1(4):041001. [PubMed: 21152382]

8. Saha AK, Kohles SS. A Cell-Matrix Model of Anabolic and Catabolic Dynamics During Cartilage Biomolecule Regulation. International Journal of Computers in Healthcare. 2011 in press.

9. Haupt JL, Frisbie DD, McIlwraith CW, Robbins PD, Ghivizzini S, Evans CH, Nixon AJ. Dual Transduction of Insulin-Like Growth Factor-I and Interleukin-1 Receptor Antagonist Protein Controls Cartilage Degradation in an Osteoarthritic Culture Model. J Orthop Res. 2005; 23:118–126. [PubMed: 15607883]

10. Loeser RF, Chubinskaya S, Pacione C, Im H. Basic Fibroblast Growth Factor Inhibits the Anabolic Activity of Insulin-Like Growth Factor I and Osteoprotein I in Adult Human Articular Cartilage Chondryocytes. Arthritis Rheum. 2005; 52:3910–3917. [PubMed: 16320338]

11. Im H-J, Muddasani P, Natarajan V, Schmid TM, Block JA, Davis F, van Wijnen AJ, Loeser RF. Basic Fibroblast Growth Factor Stimulates Matrix Metalloproteinase-13 via the Molecular Cross-Talk Between the Mitogen-Activated Protein Kinases and Protein Kinase Cδ Pathways in Human Adult Articular Chondryocytes. J Biol Chem. 2007; 282:11110–11121. [PubMed: 17311929]

12. Saha AK, Mazumdar JN, Kohles SS. Prediction of Growth Factor Effects on Engineered Cartilage Composition Using Deterministic and Stochastic Modeling. Ann Biomed Eng. 2004; 32:871–879. [PubMed: 15255217]

13. Saha AK, Mazumdar JN, Kohles SS. Dynamic Matrix Composition in Engineered Cartilage With Stochastic Supplementation of Growth Factors. Australas Phys Eng Sci Med. 2005; 28:97–104. [PubMed: 16060315]

14. Kohles SS, Wilson CG, Bonassar LJ. A Mechanical Composite Spheres Analysis of Engineered Cartilage Dynamics. ASME J Biomech Eng. 2007; 129(4):473–480.

15. Kohles SS, Liang Y, Saha AK. Volumetric Stress-Strain Analysis of Optohydrodynamically Suspended Biological Cells. ASME J Biomech Eng. 2011; 133(1):011004.

16. Wilson ZD, Kohles SS. Two-Dimensional Modeling of Nano-Mechanical Stresses-Strains in Healthy and Diseased Single-Cells During Microfluidic Manipulation. J Nanotechnol Eng Med. 2010; 1(2):021005.

17. Li J, Kwauk M. Exploring Complex Systems in Chemical Engineering—The Multi-Scale Methodology. Chem Eng Sci. 2003; 58:521–535.

18. Tikhonov AN. Systems of Differential Equations Containing Small Parameters in the Derivatives. Math USSR Sb. 1952; 31(73):575–586.

19. Gardiner, CW. Handbook of Stochastic Methods: For Physics, Chemistry and the Natural Sciences, Synergetics. Vol. 13. Springer; Berlin: 1997.

20. Li J, Fu X, Sun X, Sun T, Sheng Z. The Interaction Between Epidermal Growth Factor and Metalloproteinase Induces the Development of Sweat Glands in Human Fetal Skin. J Surg Res. 2002; 106(2):258–263. [PubMed: 12175976]

21. Wilson CG, Bonassar LJ, Kohles SS. Modeling the Dynamic Composition of Engineered Cartilage. Arch Biochem Biophys. 2002; 408:246–254. [PubMed: 12464278]

22. Klöden, PE.; Platen, E. Numerical Solution of Stochastic Differential Equations. Springer; New York: 1995.

23. Yee CS, Farewell VT, Isenberg DA, Griffiths B, Teh LS, Bruce IN, Ahmad Y, Rahman A, Prabu A, Akil M, McHugh N, Edwards C, D'Cruz D, Khamashta MA, Gordon C. The Use of Systemic Lupus Erythematosus Disease Activity Index-2000 to Define Active Disease and Minimal Clinically Meaningful Change Based on Data From a Large Cohort of Systemic Lupus Erythematosus Patients. Rheumatology. 2011; 50(5):982–988. [PubMed: 21245073]

24. Olsen NJ. Scleroderma: The Need for Extreme Remidies. Am J Med Sci. 2011 in press.

25. De Ceuninck F, Sabatini M, Pastoureau P. Recent Progress Towards Biomarker Identification in Osteoarthritis. Drug Discovery Today. 2011 in press.

26. Carantino I, Florescu IP, Carantino A. Overview About the Keloid Scars and the Elaboration of a Non-Invasive, Unconventional Treatment. Journal of Medicine and Life. 2010; 3:122–127. [PubMed: 20968196]

27. Lammi MJ. Current Prospective on Cartilage and Chondrocyte Mechanobiology. Bioreheology. 2004; 41:593–596.

28. Wheeler CA, Fitzgerald JB, Gordzinsky AJ. Cartilage Mechanobiology: The Response of Chondrocyte to Mechanical Force. Curr Opin Orthop. 2005; 16:346–353.

29. Kiviranta I, Jurvelin J, Tammi M, Säämänen AM, Helminen HJ. Weight Bearing Controls Glycosaminoglycan Concentration and Articular Cartilage Thickness in the Knee Joints of Young Beagle Dogs. Arthritis Rheum. 1987; 30:801–809. [PubMed: 3619962]

30. Helminen, HJ.; Kiviranta, I.; Säämänen, AM.; Jurvelin, JS.; Arokoski, J.; Oettmeier, R.; Abendroth, K.; Roth, AJ.; Tammi, MI. Articular Cartilage and Osteoarthritis. Kuettner, KE.; Hascall, VC.; Schleyerbach, R., editors. Raven; New York: 1992. p. 501-510.

31. Flannery CR, Hughes CE, Schumacher BL, Tudor D, Aydelotte MB, Kuettner KE, Caterson B. Articular Cartilage Superficial Zone Protein _SZP_ is Homologous to Megakaryocyte Stimulating Factor Precursor and Is a Multifunctional Proteoglycan With Potential Growth-Promoting, Cytoprotective, and Lubricating Properties in Cartilage Metabolism. Biochem Biophys Res Commun. 1999; 254:535–541. [PubMed: 9920774]

32. Roughley PJ. The Structure and Function of Cartilage Proteoglycans. Eur Cells Mater. 2006; 12:92–101.

33. Woo SL, Akeson WH, Jemmott GF. Measurements of Nonhomogeneous, Directional Mechanical Properties of Articular Cartilage in Tension. J Biomech. 1976; 9:785–791. [PubMed: 1022791]

34. Roth V, Mow VC. The Intrinsic Tensile Behavior of the Matrix of Bovine Articular Cartilage and Its Variation With Age. J Bone Jt Surg, Am. 1980; 62:1102–1117.

35. Ateshian, GA.; Mow, VC. Basic Orthopaedic Biomechanics and Mechano-Biology. Mow, VC.; Huiskes, R., editors. Lippincott Williams & Wilkins; Philadelphia: 2005. p. 447-494.
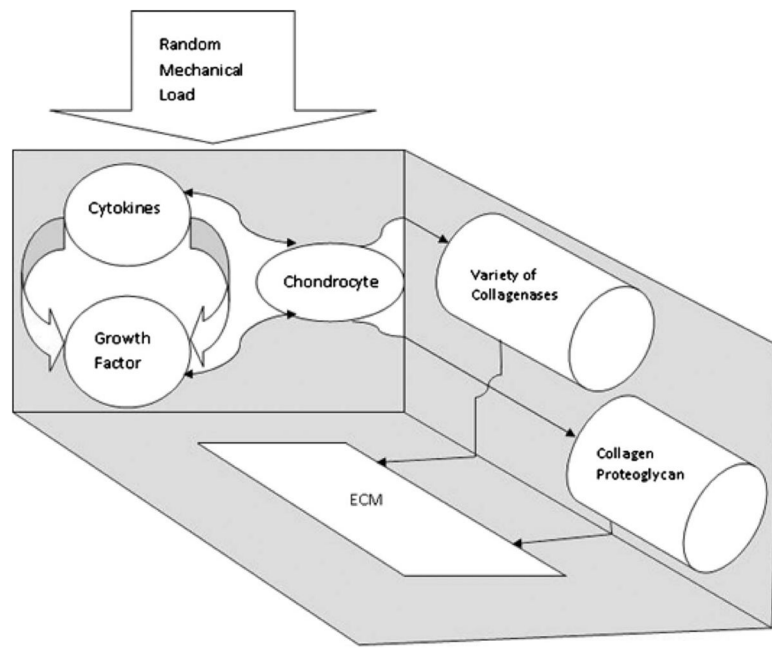
Fig. 1.
The schematic diagram of the growth factor-cytokine interaction network as they influence the structural molecules, collagen, and proteoglycans, within the ECM. The three different planes represent the three different time scales.
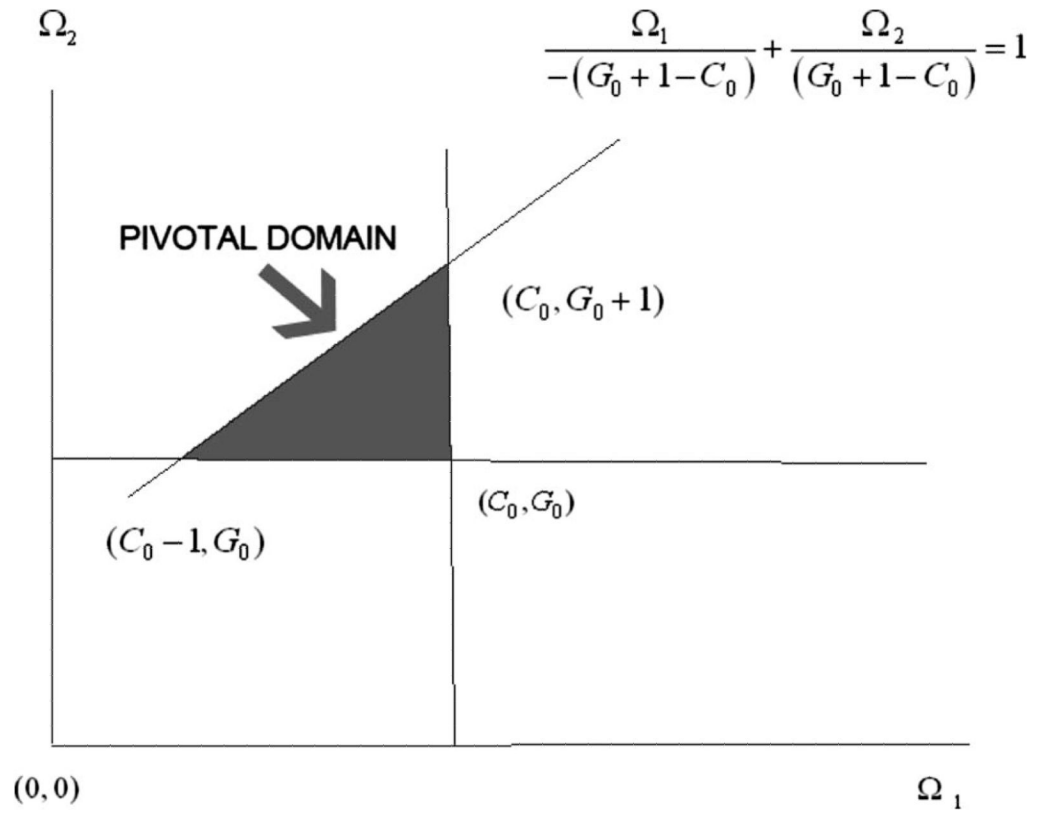
Fig. 2.
The pivotal region of the threshold parameters Ω_1 and Ω_2 are shown in the shaded area bounded by the upper bound as defined by the lower left intercept= (15.489,19.161) and the upper right intercept= (16.489,21.161), where the lower bound is $(C_0, G_0) = (16.489,19.161)$ [7]. These relationships satisfy that described in Eq. (14).
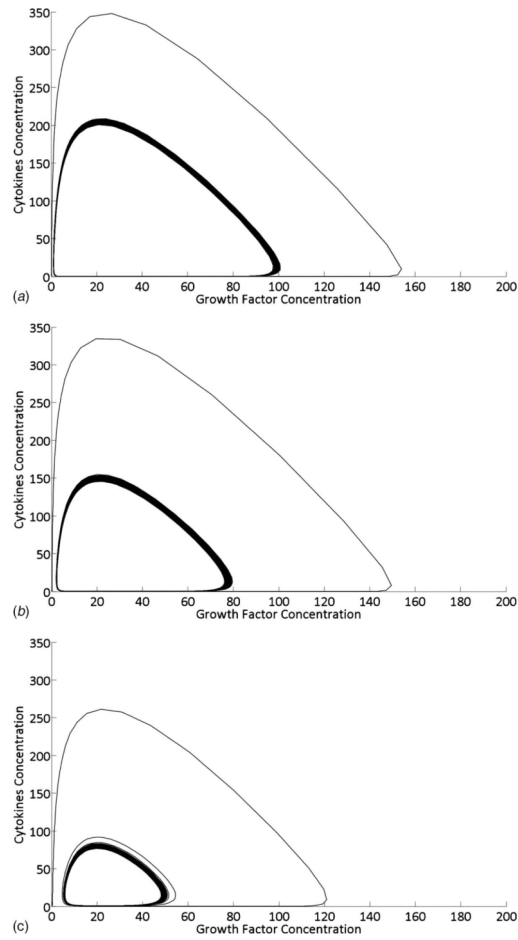
Fig. 3.
Phase-plane diagrams demonstrating the interactive dynamics of cytokines and growth factors. The stochastic function defines varying mechanical load magnitudes as the applied stimulus. A harmonic balance with a clockwise rotating limit cycle results from relative loads of (*a*) 0.001 with centering at the steady state value of $(\bar{C}, \bar{G})^T \approx (18.03, 20.95)^T$, (*b*) 0.01 with centering at the steady state value of $(\bar{C}, \bar{G})^T \approx (17.49, 20.37)^T$, and (*c*) 0.1 with centering at the steady state value of $(\bar{C}, \bar{G})^T \approx (16.51, 19.62)^T$. All concentration units are in dimensionless form.
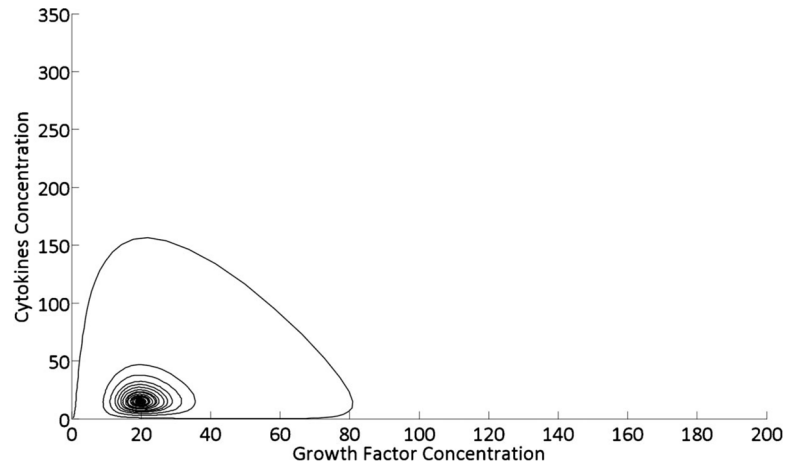
Fig. 4.
The phase-plane diagram indicating a disruption in the cyclic nature of the cytokine and growth factor dynamics due to relative loads greater than 0.5 as produced by the stochastic function. The nonoscillatory steady state now has a trajectory toward a singular value at $(\bar{C}, \bar{G})^T \approx (15.04, 19.73)^T$.
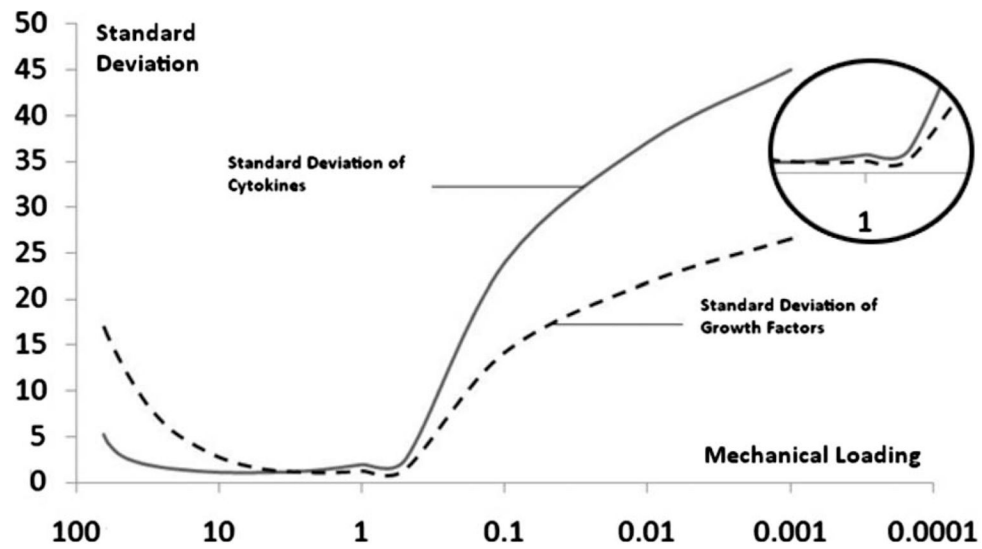
Fig. 5.
A Monte Carlo computation of the standard deviations associated with cytokine and growth factor concentrations at different dimensionless random load levels. The standard deviations appear to overlap at ~5 relative load units. The critical transition zone is identified at $1.0 \leq$ load ≤ 5.0 (see inset). Persistence in the stability of the oscillatory behavior of the anabolic and catabolic pathways toward homeostasis is possible only when random loading is less than unity. Random loading greater than 5.0 appears to help destabilize the oscillatory nature of the system, thus enhancing the growth factors to promote anabolic pathways (synthesis) over catabolism (degradation), a biologically relevant transition for tissue remodelling.
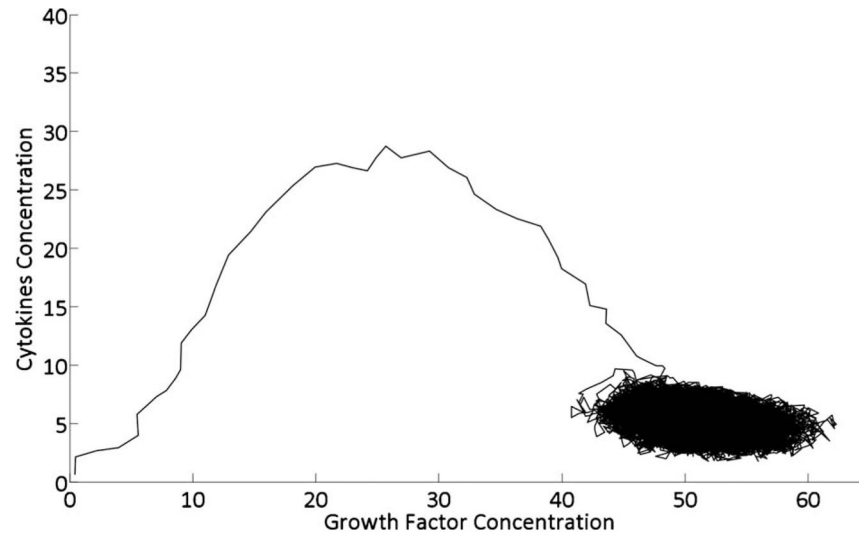
Fig. 6.
As stochastic loading increases to over 10 relative units, the harmonic balance between cytokine and growth factor activities is not visible, rather a chaotic nature is observed with a lower concentration of cytokines and a higher concentration of growth factors. The steady state value, calculated from 50,000 sample points, is given by $(\bar{C}, \bar{G})^T \approx (5.23, 51.44)^T$.
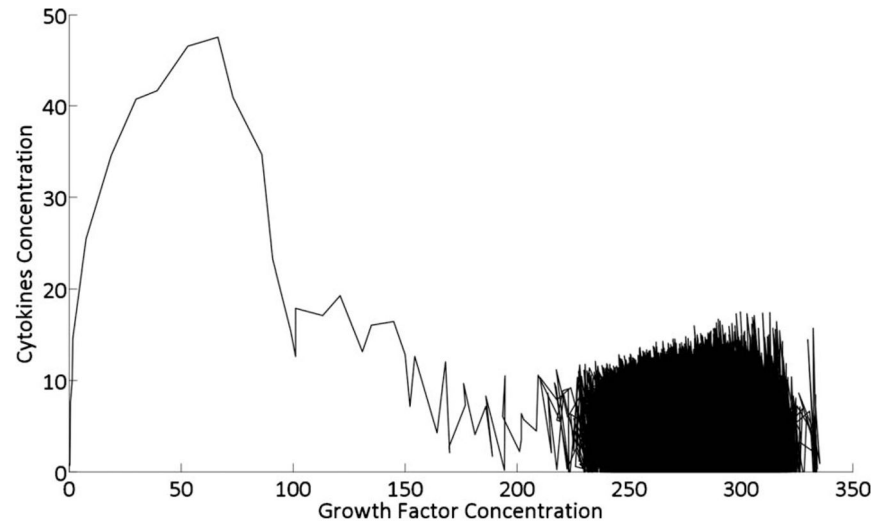
Fig. 7.
As the stochastic loading is increase above 60 relative units, a chaotic nature in the phase-plant diagram is much more aggressive with the steady state value defined at $(\bar{C}, \bar{G})^T \approx (3.91, 276.70)^T$.
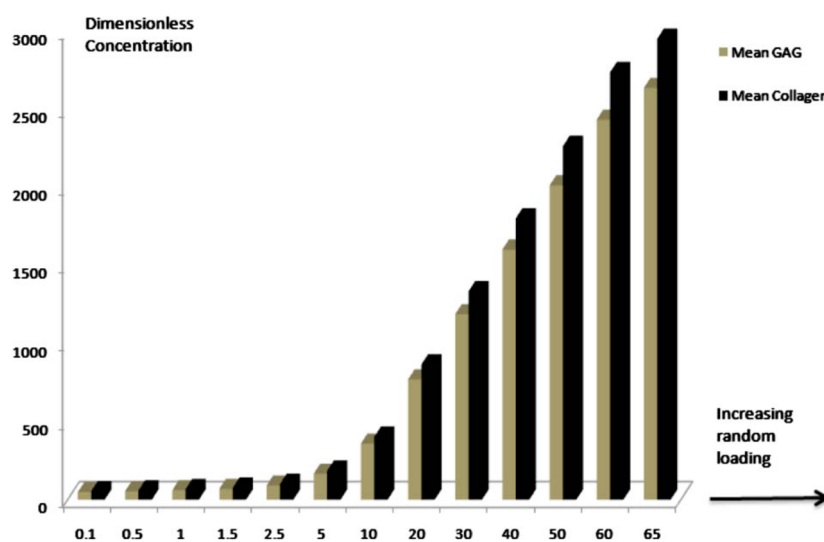
Fig. 8.
The mean dimensionless accumulation of GAG and collagen molecules within ECM as the dimensionless random mechanical loading increases from 0.1 to 65. A numerical transition in accumulation is indicated at >5.0 relative units.

Table 1

Metabolic parameters and biokinetic rates developed from a systems biology approach for describing molecular homeostatis

Parameters	Description	Relationship or Value
α_1	Synthesis rate: cytokines	$\alpha_1 = 0.048 + \beta_1$ [a]
α_2	Synthesis rate: growth factors	$\alpha_2 = 0.044 + \beta_2$ [a]
β_1	Decay rate: cytokines	$\beta_1 = \dfrac{1}{\tau_1} \left\{ \dfrac{\Omega_2 - G_0}{G_0 + 1 - \Omega_2} \right\}$ [a]
β_2	Decay rate: growth factors	$\beta_2 = \dfrac{1}{\tau_2} \left\{ \dfrac{C_0 - \Omega_1}{\Omega_1 - C_0 - 1} \right\}$ [a]
λ_1	Synthesis rate: GAG molecules	5.474×10^{-3} [b]
λ_2	Synthesis rate: collagen molecules	5.400×10^{-2} [b]
δ_1	Decay rate: GAG molecules	1.264×10^{-4} [b]
δ_2	Decay rate: collagen molecules	1.108×10^{-3} [b]
Ω_1	Threshold value: cytokines	$C_0 - 1 < \Omega_1 < C_0$ [a]
Ω_2	Threshold value: growth factors	$G_0 < \Omega_2 < G_0 + 1$ [a]
τ_1	Characteristic time: cytokines	20.7 weeks [c]
τ_2	Characteristic time: growth factors	22.9 weeks [c]

[a] From Refs. [6–8].

[b] From Ref. 13 as derived from Ref. 21.

[c] From Ref. 20.